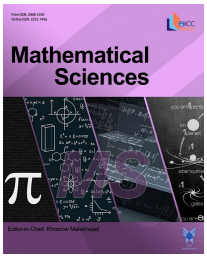

Math. Sci. 2026; 20(1): 90-107

Mathematical Sciences (MS)

https://doi.org/10.57647/mathsci.2026.2001.06

Research Article

A Robust Numerical Scheme for Three-Dimensional Time-Space Fractional PDEs Using Cubic Spline and Meshless Methods

Mousa J. Huntul *

Department of Mathematics, College of Science, Jazan University,P.O. Box. 114, Jazan 45142, Saudi Arabia

*Corresponding author: mhantool@jazanu.edu.sa

Article History

Received:
29 December 2025

Revised:
03 February 2026

Accepted:
15 February 2026

Published online:
31 March 2026

Abstract:

This paper investigates the numerical solution of a three-dimensional time–space fractional functional partial differential equation involving Caputo fractional derivatives in time and Riesz fractional derivatives in space. Owing to the inherent difficulties associated with fractional operators, such as weakly singular kernels and strong nonlocality, conventional numerical methods often encounter limitations in terms of accuracy and computational efficiency. To address these challenges, a hybrid numerical scheme is developed in which the Caputo fractional derivative is discretized by means of cubic spline interpolation, providing high-order temporal accuracy, while advanced meshless techniques are employed for the spatial approximation of the Riesz fractional derivative, thereby effectively managing its global support and singular behavior. The resulting fully discrete scheme is rigorously analyzed, and its unconditional stability is established using the energy method. Extensive numerical experiments on various three-dimensional domains demonstrate the high accuracy of the proposed method, with convergence rates consistent with the theoretical analysis, as well as favorable computational efficiency. Overall, the proposed approach offers a robust and flexible computational framework for the numerical treatment of complex fractional models arising in physics, engineering, and applied sciences.

Keywords: Stability analysis; Cubic spline discretization; Meshless numerical methods; Three-dimensional fractional PDEs; Nonlocal operators

Cite this article: M. J. Huntul A Robust Numerical Scheme for Three-Dimensional Time-Space Fractional PDEs Using Cubic Spline and Meshless Methods. Math. Sci 2026; *20*(1): 90-107 https://doi.org/10.57647/mathsci.2026.2001.06

1. Introduction

Fractional calculus has become an essential mathematical tool for the modeling of complex dynamical systems exhibiting memory effects and nonlocal interactions [1, 2, 3, 4, 5, 6, 7, 8]. In particular, the Caputo fractional derivative is extensively employed in time-fractional formulations due to its ability to incorporate initial conditions in terms of integer-order derivatives, thereby preserving physical consistency and interpretability. This operator effectively characterizes temporal memory phenomena arising in viscoelastic materials, anomalous diffusion processes, and biological systems. On the other hand, the Riesz fractional derivative serves as a symmetric and nonlocal spatial operator that generalizes the classical Laplacian and is well suited for describing anomalous transport mechanisms such as Lévy flights and turbulent diffusion, where conventional diffusion operators are inadequate. The combination of Caputo and Riesz fractional derivatives yields a comprehensive time–space fractional framework capable of capturing both long-range temporal dependence and spatial heterogeneity. Such fractional models have been successfully applied across a wide range of scientific and engineering disciplines, including physics, biology, finance, and engineering. Owing to their intrinsic nonlocality and mathematical flexibility, fractional differential operators offer improved modeling accuracy and enhanced adaptability compared with classi-

cal integer-order counterparts, particularly for systems defined on irregular geometries or heterogeneous media.

We consider the following three-dimensional time-space fractional functional partial differential equation:

$$
\begin{aligned}
{}^{C}D_t^{\beta}u(x,y,z,t) &= -\left(D_x^{\alpha}u + D_y^{\alpha}u + D_z^{\alpha}u\right) \quad (1)\\
&+\lambda(u^{p}(x,y,z,t)\\
&+\int_{\Omega} K(x,y,z,\xi,\eta,\zeta)u(\xi,\eta,\zeta,t)\,d\xi d\eta d\zeta),
\end{aligned}
$$

subject to the initial condition:

$$u(x,y,z,0) = u_0(x,y,z), \quad \forall (x,y,z) \in \Omega,$$

and the boundary condition:

$$u(x,y,z,t) = 0, \quad \forall (x,y,z) \in \partial\Omega, \quad t \in [0,T].$$

For $\beta \in (0,1)$, the Caputo fractional derivative of a function $u(t)$ is defined by:

$${}^{C}D_t^{\beta}u(t) = \frac{1}{\Gamma(1-\beta)}\int_0^t \frac{u'(\tau)}{(t-\tau)^{\beta}}\,d\tau. \quad (2)$$

This is equivalently expressed using the Riemann–Liouville integral $I^{1-\beta}$ as:

$${}^{C}D_t^{\beta}u(t) = I^{1-\beta}\left(\frac{d}{dt}u(t)\right). \quad (3)$$

For $\alpha \in (1,2)$, the Riesz fractional derivative [9] in one spatial dimension is defined via left and right Riemann–Liouville derivatives as:

$$D_x^{\alpha}u(x) = -\frac{1}{2\cos(\pi\alpha/2)}\left({}_{-\infty}D_x^{\alpha}u(x) + {}_{x}D_{\infty}^{\alpha}u(x)\right). \quad (4)$$

The left-sided and right-sided Riemann–Liouville fractional derivatives are defined by [10]:

$${}_{-\infty}D_x^{\alpha}u(x) = \frac{1}{\Gamma(n-\alpha)}\frac{d^n}{dx^n}\int_{-\infty}^{x}\frac{u(s)}{(x-s)^{\alpha-n+1}}\,ds, \quad (5)$$

$${}_{x}D_{\infty}^{\alpha}u(x) = \frac{(-1)^n}{\Gamma(n-\alpha)}\frac{d^n}{dx^n}\int_{x}^{\infty}\frac{u(s)}{(s-x)^{\alpha-n+1}}\,ds, \quad (6)$$

where $n = \lceil\alpha\rceil$ is the smallest integer greater than or equal to α. In this model, $u(x,y,z,t)$ is the unknown scalar field representing the state of the system over space and time, $\Omega \subset \mathbb{R}^3$ is the bounded spatial domain with boundary $\partial\Omega$, $t \in [0,T]$ is the time interval of interest, $\beta \in (0,1)$ is the order of the Caputo time-fractional derivative capturing memory effects, $\alpha \in (1,2)$ is the order of the Riesz space-fractional derivative representing anomalous diffusion, D_q^{α} for $q = x,y,z$ are the one-dimensional Riesz fractional derivatives in each spatial direction, $\lambda \in \mathbb{R}$ is a scalar parameter scaling the nonlinear source term, $p > 1$ is the exponent in the power-law nonlinearity, $K(x,y,z,\xi,\eta,\zeta)$ is a symmetric kernel function modeling long-range interactions across space, and $u_0(x,y,z)$ is the prescribed initial condition of the system.

Numerical methods are essential tools for solving mathematical models that cannot be treated analytically or for which exact solutions are difficult to obtain. In fractional models involving derivatives of non-integer order, analytical solutions are often complicated or unavailable due to the intrinsic memory and nonlocal properties of fractional calculus. Numerical methods provide efficient and accurate approximations of such solutions and enable the investigation of real-world phenomena described by fractional differential equations, including anomalous diffusion, viscoelastic materials, and control systems, where classical integer-order models are inadequate. By discretizing both time and space, numerical methods transform complex fractional problems into solvable algebraic systems, thereby facilitating simulation, prediction, and analysis in engineering, physics, biology, and finance. Consequently, numerical techniques are indispensable for the practical application of fractional models. Among various numerical approaches, spline-based methods have been extensively investigated. Lakestani et al. [11] developed an operational matrix of fractional derivatives using B-spline functions, providing a flexible and accurate tool for fractional problems. Similarly, Zahra and Elkholy [12] employed cubic splines to solve fractional differential equations, highlighting the effectiveness of spline approximations in fractional calculus. Advanced spline techniques have also been utilized for time-fractional nonlinear partial differential equations. Majeed et al. [13] proposed an extended cubic B-spline method for the time-fractional modified Burgers' equation, demonstrating its efficiency in nonlinear settings. More recently, Sorgentone et al. [14] introduced a spline-based framework for space–time fractional convection–diffusion problems, further extending the applicability of spline methods to multidimensional fractional models. Isogeometric analysis (IGA) has emerged as a powerful numerical approach for fractional partial differential equations. Ge et al. [15] developed space–time continuous and time-discontinuous Galerkin schemes based on IGA to accurately capture the nonlinear dynamics of time-fractional equations. Earlier, Feng et al. [16] investigated numerical methods for forward and backward problems in time–space fractional diffusion equations, emphasizing the necessity of robust schemes for inverse problems. Shifted polynomial collocation techniques have been proposed for multidimensional fractional partial differential equations. Anjuman et al. [17] applied the shifted Legendre–Gauss–Lobatto collocation method to a three-dimensional time–space fractional reaction–advection–diffusion equation, achieving high accuracy with spectral convergence. Within the framework of finite difference methods, Zhao et al. [18] presented a fast finite difference scheme for three-dimensional time-dependent space-fractional diffusion equations with fractional derivative boundary conditions, significantly reducing computational cost. Wang et al. [19] introduced an alternating-direction implicit spectral Galerkin method for multi-term fractional

10.57647/mathsci.2026.2001.06

diffusion problems in three dimensions, addressing the challenges associated with high-dimensional fractional operators. Meshfree and particle-based methods have also been employed for the numerical solution of fractional partial differential equations. Lin et al. [4] proposed a reproducing kernel particle method for irregular domains, illustrating the flexibility of meshfree techniques. Bohaienko [20] developed parallel finite difference algorithms for space-fractional diffusion equations with ψ-Caputo derivatives, enhancing computational efficiency in high-dimensional settings. Zhu et al. [21] further advanced meshless approaches for high-dimensional multi-term time–space fractional partial differential equations on convex domains. Finite volume and generalized finite difference methods have been investigated for handling space-fractional operators. Zhang et al. [22] introduced a vertex-centered finite volume method for multi-term fractional Bloch–Torrey equations, while Sun et al. [23] proposed a generalized finite difference method for multidimensional space-fractional diffusion equations. Polynomial-based high-order schemes and Lagrange polynomial methods provide effective alternatives for distributed-order fractional models. Ghoreyshi et al. [24] developed two high-order numerical schemes based on Lagrange polynomials for time-fractional partial integro-differential equations on non-rectangular domains, ensuring both high accuracy and numerical stability.

Hybrid numerical methods have been proposed for fractional diffusion models involving Caputo and Riesz derivatives. Derakhshan et al. [2] presented a hybrid scheme with high accuracy for solving time-space fractional diffusion models, combining spatial discretization techniques with fractional time operators. Mixed finite element methods are useful for higher-order time-fractional models with Riesz space-fractional derivatives of distributed order. Irandoust-Pakchin and Derakhshan [3] investigated such methods with stability analysis, proving their effectiveness in complex fractional PDEs. Optimal solvers and preconditioning techniques have been developed for two-dimensional Riesz space fractional nonlinear reaction-diffusion equations. Qu et al. [25] proposed a novel fourth-order scheme combined with optimal preconditioners to enhance convergence rates. For fractional advection-diffusion equations, Shahbazi et al. [26] introduced fractional exponential fitting and adapted backward differentiation formula (BDF) methods, improving numerical stability and accuracy. Earlier foundational works by Yang et al. [27] and Ray and Sahoo [28] laid important groundwork in numerical methods for fractional PDEs with Riesz space derivatives and analytical approximate solutions respectively, influencing subsequent numerical algorithm developments. Meshless methods have received considerable attention due to their flexibility in complex geometries and irregular domains. Owolabi and Atangana [29] solved nonlinear Schrödinger equations with Riesz derivatives using meshless methods. Shen et al. [30] investigated fundamental and numerical solutions of Riesz fractional advection-dispersion equations. Yuan et al. [31] advanced numerical modeling of Riesz space fractional advection–dispersion equations with meshfree approaches, providing accurate results in high-dimensional problems. Improved numerical methods for Riesz space fractional PDEs were developed by Rahman et al. [32], focusing on feasibility and accuracy. Nguyen et al. [33] reviewed meshless methods comprehensively, discussing implementation aspects and practical considerations. The enforcement of essential boundary conditions in meshless approximations using finite elements was studied by Krongauz and Belytschko [34], while Shivanian [35] applied meshless local Petrov–Galerkin methods to nonlinear wave equations with moving least squares approximation. Li [36] proposed meshless Galerkin algorithms for boundary integral equations, demonstrating the versatility of meshfree techniques in integral formulations. Atluri et al. [1] analyzed thin beams using meshless local Petrov–Galerkin methods with generalized moving least squares interpolations, extending meshless applications to structural mechanics. Assari et al. [5] developed meshless methods based on moving least squares for nonlinear integral equations on non-rectangular domains, emphasizing robustness in complex geometries. Chowdhury et al. [37] proposed an element-free Galerkin method based on modified moving least squares approximations, enhancing numerical stability and accuracy.

Recent advances in numerical methods for fractional and nonlocal models have significantly improved the accuracy and efficiency of simulations in applied mathematics. Luo et al. [38] developed a second-order accurate, robust, and efficient ADI Galerkin technique for solving three-dimensional nonlocal heat models arising in viscoelasticity. This method demonstrated superior stability compared to traditional approaches. Efficient alternating direction implicit (ADI) methods have also been explored for distributed-order fractional integro-differential equations. Guo et al. [39] proposed numerical schemes that reduce computational cost while maintaining high accuracy for multi-dimensional problems. Similarly, Qiu et al. [40] investigated generalized tempered-type integrodifferential equations, highlighting the flexibility of their approach with respect to varying kernel functions. In the context of nonlinear fractional wave models, Nikan et al. [41] conducted a detailed numerical simulation of the fractional regularized long-wave equation relevant to ion acoustic plasma waves. Moreover, for financial applications, Nikan et al. [42] introduced an improved local radial basis function method for pricing options under the time-fractional Black–Scholes model, showing its practical effectiveness in quantitative finance. Additionally, the study of fractional fluid dynamics has seen notable contributions. Nikan et al. [43] presented a numerical solution for the fractional Rayleigh–Stokes model in a heated generalized second-grade fluid, illustrating the capability of fractional models to capture complex flow behavior.

Nikan et al. [44] also proposed a numerical approach for pricing American and European options using a time-fractional Black–Scholes model, demonstrating its effectiveness in financial decision-making. Overall, these works collectively demonstrate the growing importance of robust and efficient numerical methods in addressing fractional, nonlocal, and integro-differential problems in various scientific and engineering fields.

The incorporation of Caputo fractional derivatives in time and Riesz fractional derivatives in space introduces intrinsic nonlocal behavior and singular kernels, which pose significant challenges for both analytical and numerical solutions. Conventional numerical methods often encounter limitations in accuracy and efficiency when addressing these complexities, particularly in three-dimensional domains with irregular geometries. To overcome these obstacles, the present study develops a hybrid numerical scheme that combines cubic spline interpolation in time with meshless spatial discretization. The cubic spline approach ensures high-order temporal accuracy for the Caputo fractional derivative, capturing the memory effects inherent in fractional dynamics with minimal discretization error. Simultaneously, the meshless method provides a flexible and accurate approximation of the Riesz fractional derivative, effectively managing its global support and singular behavior without the need for structured meshes. While cubic spline and meshless techniques have been investigated individually in the context of fractional partial differential equations, the novelty of the proposed framework lies in their rigorous integration into a fully discrete scheme. This unified approach allows for simultaneous control over temporal and spatial discretization errors, leading to enhanced stability and provable convergence. Furthermore, the method is well-suited to handle nonlinear terms and nonlocal interactions represented by integral kernels, which frequently appear in fractional functional PDEs. The combination of high-order temporal accuracy, precise spatial approximation, and theoretical convergence guarantees distinguishes this work from existing spline-based or meshless schemes, offering a robust and efficient tool for solving complex three-dimensional fractional problems. Numerical experiments confirm the method's reliability, efficiency, and potential applicability across a broad class of fractional functional equations.

The rest of this manuscript is summarized and concluded as follows. In Section 2, we introduce a novel discretization technique for the Caputo fractional derivative based on cubic spline interpolation. This approach enhances temporal accuracy and provides a smooth representation of the solution in time. In Section 3, we construct a meshless discretization method for the Riesz fractional derivative, leveraging radial basis functions to avoid the limitations of grid-based schemes and effectively capture spatial nonlocality. In Section 4, we develop a fully discrete numerical scheme by combining the cubic spline and meshless approximations. This integrated framework facilitates the efficient and flexible simulation of the time–space fractional model. In Section 5, we rigorously analyze the convergence properties of the proposed scheme and establish its numerical stability under appropriate assumptions. Theoretical results guarantee that the method reliably approximates the true solution as discretization parameters are refined. In Section 6, we present a series of numerical experiments to validate the performance of the proposed method. The results confirm the schemes accuracy, convergence order, and ability to handle various fractional parameters and nonlinearities. Finally, in Section 7, we summarize the main findings, highlight the advantages of the proposed method, and outline potential directions for future research in fractional differential equations.

2. Discretization of Caputo Fractional Derivative Using Cubic Spline

In this section, we construct a high-order discretization of the Caputo fractional derivative based on cubic spline interpolation in time. Consider a uniform time grid $\{t_j\}_{j=0}^{N}$ with step size Δt, and denote $u_j = u(t_j)$. Let $S(t)$ be the natural cubic spline that interpolates the function $u(t)$ at the nodes $\{t_j\}$. On each subinterval $[t_{j-1}, t_j]$, the spline $S(t)$ takes the form:

$$S(t) = a_j + b_j(t - t_{j-1}) + c_j(t - t_{j-1})^2 + d_j(t - t_{j-1})^3,$$

where the coefficients a_j, b_j, c_j, d_j are determined by the interpolation conditions $S(t_j) = u_j$, $S(t_{j-1}) = u_{j-1}$, and the continuity of the first and second derivatives across the grid points. The natural spline boundary conditions impose that the second derivative vanishes at the endpoints, i.e.,

$$S''(t_0) = S''(t_N) = 0.$$

In this work, we denote by $C^4([0,T])$ the space of functions $u : [0,T] \to \mathbb{R}$ that are four times continuously differentiable with respect to time t, i.e.,

$$u \in C^4([0,T]) \iff u, u', u'', u''', u'''' \text{ exist and are continuous on } [0,T].$$

Similarly, $C^{3,2}([0,T] \times \Omega)$ denotes the space of functions $u : [0,T] \times \Omega \to \mathbb{R}$ that are three times continuously differentiable with respect to time t and twice continuously differentiable with respect to the spatial variables $(x, y, z) \in \Omega$, that is,

$$u \in C^{3,2}([0,T] \times \Omega) \iff \frac{\partial^m u}{\partial t^m}, \frac{\partial^\ell u}{\partial x^i \partial y^j \partial z^k} \text{ exist and are continuous for } m \le 3,\ i + j + k \le 2.$$

These smoothness assumptions ensure the validity of the high-order temporal and spatial discretizations used in the cubic spline and meshless methods, respectively. For consistency, we assume throughout the theoretical analysis that the exact solution u belongs to $C^{3,2}([0,T]\times\Omega)$, which provides sufficient regularity for

10.57647/mathsci.2026.2001.06

error estimation while encompassing the requirements of time derivatives up to third order and spatial derivatives up to second order.

Theorem 2.1 *Let $u(x,y,z,t)$ be sufficiently smooth with respect to time on the interval $[0,T]$ for each fixed spatial point $(x,y,z) \in \Omega$, and let $S_t(t)$ be the natural cubic spline interpolant of $u(x,y,z,t)$ at the discrete time nodes $\{t_k\}_{k=0}^n$, with uniform time step Δt. Then, the Caputo fractional derivative of order $0<\beta<1$ at time $t=t_n$ can be approximated by*

$$ {}^{C}D_t^{\beta} u(x,y,z,t_n) \approx \frac{1}{\Gamma(1-\beta)} \sum_{j=1}^{n} \Big[b_j \theta_j B_j^{(0)} + 2c_j \theta_j^2 B_j^{(1)} + 3d_j \theta_j^3 B_j^{(2)} \Big] + O(\Delta t^{2-\beta}), \tag{7} $$

where $S_t'(t) = b_j + 2c_j(t-t_{j-1}) + 3d_j(t-t_{j-1})^2$ is the derivative of the cubic spline over the interval $[t_{j-1},t_j]$, $\theta_j = t_n - t_{j-1}$, and $B_j^{(k)} = \int_0^{\Delta t/\theta_j} \frac{z^k}{(1-z)^{\beta}}\, dz$ for $k=0,1,2$. The approximation yields an error of order $O(\Delta t^{2-\beta})$, provided that $u \in C^4([0,T])$.

Proof: We start from the spline-based approximation of the Caputo fractional derivative at time t_n:

$$ {}^{C}D_t^{\beta} u(x,y,z,t_n) = \frac{1}{\Gamma(1-\beta)} \sum_{j=1}^{n} \int_{t_{j-1}}^{t_j} \frac{S_t'(t)}{(t_n-t)^{\beta}}\, dt + R_n, $$

where $S_t(t)$ is the natural cubic spline interpolant of $u(x,y,z,t)$, $S_t'(t)$ its derivative, and R_n denotes the local truncation error of the spline-based approximation, satisfying

$$ |R_n| = O(\Delta t^{2-\beta}). $$

On each subinterval $[t_{j-1},t_j]$, the spline derivative is given by

$$ S_t'(t) = b_j + 2c_j(t-t_{j-1}) + 3d_j(t-t_{j-1})^2, $$

with coefficients b_j, c_j, d_j determined from the spline construction. Defining

$$ \theta_j = t_n - t_{j-1}, $$

and substituting the variable

$$ \xi = t - t_{j-1}, $$

so that $\xi \in [0,\Delta t]$, we have

$$ t = \xi + t_{j-1}, \quad t_n - t = \theta_j - \xi, \quad dt = d\xi, $$

and the integral becomes

$$ \int_{t_{j-1}}^{t_j} \frac{S_t'(t)}{(t_n-t)^{\beta}} dt = \int_0^{\Delta t} \frac{b_j + 2c_j\xi + 3d_j\xi^2}{(\theta_j-\xi)^{\beta}}\, d\xi. $$

This integral splits into three parts:

$$ \int_0^{\Delta t} \frac{b_j + 2c_j\xi + 3d_j\xi^2}{(\theta_j-\xi)^{\beta}} d\xi = b_j \int_0^{\Delta t} \frac{1}{(\theta_j-\xi)^{\beta}} d\xi + 2c_j \int_0^{\Delta t} \frac{\xi}{(\theta_j-\xi)^{\beta}} d\xi + 3d_j \int_0^{\Delta t} \frac{\xi^2}{(\theta_j-\xi)^{\beta}} d\xi. $$

Introducing the change of variables

$$ z = \frac{\xi}{\theta_j} \implies \xi = z\theta_j, \quad d\xi = \theta_j dz, $$

we get

$$ \theta_j - \xi = \theta_j(1-z), $$

$$ \int_0^{\Delta t} \frac{\xi^k}{(\theta_j-\xi)^{\beta}} d\xi = \theta_j^{k+1} \int_0^{\Delta t/\theta_j} \frac{z^k}{(1-z)^{\beta}} dz = \theta_j^{k+1} B_j^{(k)}, $$

for $k=0,1,2$. Hence, the integral on $[t_{j-1},t_j]$ becomes

$$ \int_{t_{j-1}}^{t_j} \frac{S_t'(t)}{(t_n-t)^{\beta}} dt = b_j\theta_j B_j^{(0)} + 2c_j\theta_j^2 B_j^{(1)} + 3d_j\theta_j^3 B_j^{(2)}. $$

Summing over all subintervals $j=1,\ldots,n$ and including the truncation error R_n, we obtain

$$ {}^{C}D_t^{\beta} u(x,y,z,t_n) = \frac{1}{\Gamma(1-\beta)} \sum_{j=1}^{n} \Big[b_j \theta_j B_j^{(0)} + 2c_j \theta_j^2 B_j^{(1)} + 3d_j \theta_j^3 B_j^{(2)} \Big] + O(\Delta t^{2-\beta}). $$

This completes the proof.

The semi-discrete numerical method approximates the Caputo fractional time derivative by employing cubic spline interpolation, as detailed in Theorem 2.1. This approach effectively transforms the fractional integral into a weighted sum of spline coefficients. Consequently, it eliminates the need for direct evaluation of temporal integrals, converting the problem into a system of discrete time equations. Meanwhile, the spatial fractional derivatives and nonlinear terms are preserved in their continuous form. This simplification allows the numerical method to focus on computations at discrete time levels, facilitating efficient and accurate time stepping. Thus, the fully discrete scheme can be expressed as

$$ \frac{1}{\Gamma(1-\beta)} \sum_{j=1}^{n} \Big[b_j \theta_j B_j^{(0)} + 2c_j \theta_j^2 B_j^{(1)} + 3d_j \theta_j^3 B_j^{(2)} \Big] = -\big(D_x^{\alpha} u^n + D_y^{\alpha} u^n + D_z^{\alpha} u^n \big) + \lambda \left((u^n)^p + \int_{\Omega} K(x,y,z,\xi,\eta,\zeta) u^n(\xi,\eta,\zeta)\, d\xi d\eta d\zeta \right). $$

Theorem 2.2 *Let $u(x,y,z,t)$ be the exact solution of Eq. (1) with sufficiently smooth initial and boundary data. Assume u^n is the numerical solution obtained from the semi-discrete scheme defined by the cubic spline discretization of the Caputo fractional derivative as in Equation (8). Then, there exists a constant $C>0$, independent of the time step Δt, such that the error $e^n = u(t_n) - u^n$ satisfies*

$$ \|e^n\| \le C(\Delta t)^{2-\beta}, \quad 0<\beta<1. $$

10.57647/mathsci.2026.2001.06

Proof: Define the error function at time t_n as $e^n = u(t_n) - u^n$, where $u(t_n)$ is the exact solution and u^n is the numerical approximation. The semi-discrete fractional derivative operator $\mathcal{D}^{\beta}_{\text{num}}$, constructed via cubic spline interpolation, approximates the Caputo fractional derivative. Applying it to the exact solution, we write

$$ {}^{C}D^{\beta}_{t}u(t_n) = \mathcal{D}^{\beta}_{\text{num}}u(t_n) + R^n,$$

where R^n denotes the local truncation error arising from the spline approximation. From the theory of spline approximations for fractional derivatives, it is known that the truncation error satisfies the bound

$$\|R^n\| \le C(\Delta t)^{2-\beta},$$

where C is a positive constant independent of Δt, and $0 < \beta < 1$ is the fractional order in time. Next, consider the semi-discrete numerical scheme applied to the approximate solution u^n. Subtracting this scheme from the above expression yields the error equation as follows:

$$\begin{aligned}\mathcal{D}^{\beta}_{\text{num}}e^n &= -\big(D^{\alpha}_{x}e^n + D^{\alpha}_{y}e^n + D^{\alpha}_{z}e^n\big)\\ &+\lambda\left(u^p(t_n) - (u^n)^p + \int_{\Omega} K(\cdot)\big(u(t_n) - u^n\big)\right) + R^n.\end{aligned}$$

To analyze the error, we take the inner product in the Hilbert space $L^2(\Omega)$ with the error function e^n, then

$$\begin{aligned}\langle \mathcal{D}^{\beta}_{\text{num}}e^n, e^n\rangle &= -\sum_{\eta=x,y,z}\langle D^{\alpha}_{\eta}e^n, e^n\rangle\\ &+\lambda\langle u^p(t_n) - (u^n)^p, e^n\rangle\\ &+\lambda\left\langle \int_{\Omega} K(\cdot)(u(t_n) - u^n), e^n\right\rangle + \langle R^n, e^n\rangle.\end{aligned}$$

Since the Riesz fractional derivatives D^{α}_{η} are known to be self-adjoint and positive semi-definite operators, it follows that

$$\langle D^{\alpha}_{\eta}e^n, e^n\rangle \ge 0.$$

Consequently,

$$-\sum_{\eta}\langle D^{\alpha}_{\eta}e^n, e^n\rangle \le 0,$$

which contributes a non-positive term to the error evolution. Next, consider the nonlinear terms. By the local Lipschitz continuity of the function $f(u) = u^p$, there exists a constant $L_p > 0$ such that

$$\|u^p(t_n) - (u^n)^p\| \le L_p\|e^n\|.$$

Similarly, assuming the integral operator defined by the kernel K is bounded with operator norm M_K, we have

$$\left\|\int_{\Omega} K(\cdot)(u(t_n) - u^n)\right\| \le M_K\|e^n\|.$$

Using these bounds, the nonlinear inner product terms satisfy

$$\begin{aligned}\lambda\langle u^p(t_n) - (u^n)^p, e^n\rangle + \lambda\left\langle \int_{\Omega} K(\cdot)(u(t_n) - u^n), e^n\right\rangle\\ \le \lambda(L_p + M_K)\|e^n\|^2.\end{aligned}$$

Regarding the discrete fractional derivative operator, it can be shown that

$$\langle \mathcal{D}^{\beta}_{\text{num}}e^n, e^n\rangle \ge \frac{1}{2}\mathcal{D}^{\beta}_{\text{num}}\|e^n\|^2,$$

where

$$\mathcal{D}^{\beta}_{\text{num}}\|e^n\|^2 := \frac{1}{\Gamma(1-\beta)}\sum_{j=1}^{n} w_{j,n}\big(\|e^j\|^2 - \|e^{j-1}\|^2\big)$$

is a positive definite discrete fractional difference quotient that generalizes the classical difference quotient to fractional order β. Combining all inequalities, we have

$$\frac{1}{2}\mathcal{D}^{\beta}_{\text{num}}\|e^n\|^2 \le \lambda(L_p + M_K)\|e^n\|^2 + \langle R^n, e^n\rangle.$$

To handle the term involving the truncation error, apply the Cauchy–Schwarz inequality, thus

$$\langle R^n, e^n\rangle \le \|R^n\|\|e^n\|.$$

Then applying Young's inequality for any $\epsilon > 0$, we have

$$\|R^n\|\|e^n\| \le \frac{1}{2\epsilon}\|R^n\|^2 + \frac{\epsilon}{2}\|e^n\|^2.$$

Setting $\epsilon = 1$ for simplicity, we get:

$$\langle R^n, e^n\rangle \le \frac{1}{2}\|R^n\|^2 + \frac{1}{2}\|e^n\|^2.$$

Hence,

$$\mathcal{D}^{\beta}_{\text{num}}\|e^n\|^2 \le 2\lambda(L_p + M_K)\|e^n\|^2 + \|R^n\|^2 + \|e^n\|^2,$$

or equivalently,

$$\mathcal{D}^{\beta}_{\text{num}}\|e^n\|^2 \le C_1\|e^n\|^2 + C_2\|R^n\|^2,$$

where

$$C_1 = 2\lambda(L_p + M_K) + 1, \quad C_2 = 1.$$

Finally, applying the discrete fractional Grönwall inequality, which states that for any sequence y^n satisfying

$$\mathcal{D}^{\beta}_{\text{num}}y^n \le C_1 y^n + C_2(\Delta t)^{2m},$$

with constants $C_1, C_2 > 0$ and $m > 0$, it follows that

$$y^n \le C\,(\Delta t)^{2m}$$

for some constant C independent of n and Δt. Also,

$$m = 2 - \beta.$$

Taking the square root, we obtain

$$\|e^n\| \le C(\Delta t)^m,$$

which demonstrates that the semi-discrete scheme converges in time with order $m = 2 - \beta$.

10.57647/mathsci.2026.2001.06

3. Discretization of the Riesz Fractional Derivative Using Meshless Method

The Riesz fractional derivative plays a fundamental role in modeling anomalous diffusion phenomena in multi-dimensional domains, especially within the context of fractional partial differential equations (PDEs). It is defined as the symmetric combination of the left and right Riemann–Liouville fractional derivatives, which makes it inherently nonlocal in nature. Discretizing the Riesz derivative using traditional mesh-based methods can be particularly challenging due to the presence of singular kernels and its global support characteristics. In contrast, meshless methods provide a flexible and efficient alternative by approximating derivatives through scattered nodes, eliminating the need for mesh connectivity. Among these meshless techniques, moving least squares (MLS) approximations are widely used, as they enable localized and smooth representations of fractional operators, facilitating accurate and stable numerical solutions.

For bounded domains $[a, b]$, the truncated form of Eq. (4) is given by:

$$D_x^\alpha u(x) = -\frac{1}{2\cos\left(\frac{\pi\alpha}{2}\right)}\left({}_aD_x^\alpha u(x) + {}_xD_b^\alpha u(x)\right). \quad (8)$$

The left Riemann–Liouville fractional derivative is defined as:

$${}_aD_x^\alpha u(x) = \frac{1}{\Gamma(n-\alpha)}\frac{d^n}{dx^n}\int_a^x \frac{u(s)}{(x-s)^{\alpha-n+1}}\,ds, \quad (9)$$

and the right Riemann–Liouville fractional derivative is defined as:

$${}_xD_b^\alpha u(x) = \frac{(-1)^n}{\Gamma(n-\alpha)}\frac{d^n}{dx^n}\int_x^b \frac{u(s)}{(s-x)^{\alpha-n+1}}\,ds, \quad (10)$$

in which $n = \lceil\alpha\rceil$. Using quadrature and interpolation techniques, we approximate the integrals given by Eqs. (9) and (10) as follows:

$$\begin{aligned} {}_aD_x^\alpha u(x_i) &\approx \sum_{j=1}^{N} w_j^{(L)}(x_i)u(x_j), \quad (11)\\ {}_xD_b^\alpha u(x_i) &\approx \sum_{j=1}^{N} w_j^{(R)}(x_i)u(x_j), \end{aligned}$$

in which$w_j^{(L)}$ and $w_j^{(R)}$ are fractional weights obtained using a meshless kernel approximation, typically computed via Gauss–Jacobi quadrature. In a meshless method, the function $u(x)$ is approximated by

$$u(x) \approx \sum_{j=1}^{N} \phi_j(x)\,u(x_j),$$

where the shape functions $\phi_j(x)$ (such as radial basis functions or moving least squares kernels) satisfy the interpolation property $\phi_j(x_i) = \delta_{ij}$. The fractional derivative at the node x_i is then approximated as:

$$D_x^\alpha u(x_i) \approx -\frac{1}{2\cos\left(\frac{\pi\alpha}{2}\right)}\sum_{j=1}^{N}\left(w_j^{(L)}(x_i) + w_j^{(R)}(x_i)\right)u(x_j), \quad (12)$$

which leads to the compact matrix form

$$D_x^\alpha u \approx -\frac{1}{2\cos\left(\frac{\pi\alpha}{2}\right)}Wu,$$

where $W \in \mathbb{R}^{N\times N}$ is the weight matrix with entries

$$W_{ij} = w_j^{(L)}(x_i) + w_j^{(R)}(x_i).$$

The implementation of the proposed meshless scheme relies critically on the choice of radial basis functions (RBFs), the size of the support domains, and the construction of the discrete weight matrices. Let $\{x_i\}_{i=1}^N$ denote the set of spatial nodes in the domain Ω. For each node x_i, we define a local support domain Ω_i containing its neighboring nodes. The function $u(x)$ is approximated locally using a linear combination of radial basis functions $\phi(\|x - x_j\|)$ centered at the nodes $x_j \in \Omega_i$:

$$u(x) \approx \sum_{j\in\Omega_i} \lambda_j\,\phi(\|x - x_j\|),$$

where the coefficients λ_j are determined by enforcing interpolation conditions at the neighboring nodes. The discrete Riesz fractional derivative in the x-direction at node x_i is then approximated by

$$D_x^\alpha u(x_i) \approx \sum_{j\in\Omega_i} W_{ij}^{(x)}\,u(x_j),$$

where $W_{ij}^{(x)}$ are the meshless weights computed from the RBF interpolation and depend on the chosen support size and the RBF type. Analogous expressions hold for the y- and z-directions. The stability and accuracy of the scheme strongly depend on the conditioning of the weight matrices $W^{(x)}, W^{(y)}, W^{(z)}$. Therefore, it is important to select the RBF type (e.g., Gaussian, multiquadric) and the support size to balance approximation accuracy and numerical stability. In practice, compactly supported RBFs with moderate support radii are often preferred to ensure sparsity in the weight matrices and reduce computational cost. By explicitly stating these choices, the approximation of the Riesz fractional derivatives can be written in a compact matrix-vector form:

$$\mathbf{D}_x^\alpha\mathbf{u} \approx W^{(x)}\mathbf{u}, \quad \mathbf{D}_y^\alpha\mathbf{u} \approx W^{(y)}\mathbf{u}, \quad \mathbf{D}_z^\alpha\mathbf{u} \approx W^{(z)}\mathbf{u},$$

where $\mathbf{u} = [u(x_1), u(x_2), \ldots, u(x_N)]^\top$ is the vector of nodal values. This formulation highlights both the locality and the global influence of the meshless approximation, providing a clear framework for the implementation, reproducibility, and numerical analysis of the proposed scheme. The full three-dimensional Riesz fractional derivative is given by

$$D^\alpha u(x, y, z) = D_x^\alpha u + D_y^\alpha u + D_z^\alpha u.$$

10.57647/mathsci.2026.2001.06

We discretize each spatial direction independently using the meshless approach which is defined in Eq. (12), yielding

$$D^{\alpha}u(x_i,y_i,z_i) \approx \tag{13}$$
$$-\frac{1}{2\cos\left(\frac{\pi\alpha}{2}\right)}\sum_{j=1}^{N}\left(w_j^{(x)}+w_j^{(y)}+w_j^{(z)}\right)u(x_j,y_j,z_j),$$

where $W^{(x)}$, $W^{(y)}$, and $W^{(z)}$ are the directional weight matrices constructed analogously to the one-dimensional case. Thus, the discrete meshless approximation can be compactly expressed as

$$D^{\alpha}u(x_i,y_i,z_i) \approx \tag{14}$$
$$-\frac{1}{2\cos\left(\frac{\pi\alpha}{2}\right)}\sum_{j=1}^{N}\left(W_{ij}^{(x)}+W_{ij}^{(y)}+W_{ij}^{(z)}\right)u(x_j,y_j,z_j),$$

where each $W_{ij}^{(\cdot)}$ represents the fractional weight corresponding to the respective spatial direction.

4. Fully Discrete Scheme via Meshless Approximation of the Riesz Derivative

To achieve a fully discrete numerical scheme, we discretize the spatial fractional derivatives in the semi-discrete equation (8) using a meshless method. As described in Section 3, the three-dimensional Riesz fractional derivative is approximated by direction-wise meshless weights derived from moving least squares (MLS) approximations. This approach is especially effective for irregular domains and non-uniform node distributions, allowing spatial operators to be discretized without relying on structured meshes.

By substituting the meshless approximations of the Riesz fractional derivatives $D_x^{\alpha}u^n$, $D_y^{\alpha}u^n$, and $D_z^{\alpha}u^n$ into the semi-discrete equation (8), we obtain the following fully discrete formulation:

$$\frac{1}{\Gamma(1-\beta)}\sum_{j=1}^{n}\left[b_j\theta_j B_j^{(0)}+2c_j\theta_j^2B_j^{(1)}+3d_j\theta_j^3B_j^{(2)}\right] \tag{15}$$
$$=-\frac{1}{2\cos\left(\frac{\pi\alpha}{2}\right)}\sum_{k=1}^{N}\left(W_{ik}^{(x)}+W_{ik}^{(y)}+W_{ik}^{(z)}\right)u_k^n+$$
$$\lambda\left((u_i^n)^p+\int_{\Omega}K(x_i,y_i,z_i,\xi,\eta,\zeta)u^n(\xi,\eta,\zeta)\,d\xi d\eta d\zeta\right),$$

in which $u_i^n \approx u(x_i,y_i,z_i,t_n)$ denotes the numerical approximation at node i and time step n. The terms $W_{ik}^{(x)}$, $W_{ik}^{(y)}$, and $W_{ik}^{(z)}$ represent the meshless weights associated with the Riesz fractional derivatives in the x-, y-, and z-directions, respectively. Additionally, $\theta_j = t_n - t_j$, and the coefficients b_j, c_j, and d_j arise from the Caputo time discretization using cubic spline interpolation. The volume integral in the nonlocal nonlinear term can be efficiently approximated using quadrature rules as

$$\int_{\Omega}K(x_i,y_i,z_i,\xi,\eta,\zeta)\,u^n(\xi,\eta,\zeta)\,d\xi\,d\eta\,d\zeta \tag{16}$$
$$\approx\sum_{k=1}^{N}\omega_k\,K(x_i,y_i,z_i,x_k,y_k,z_k)\,u_k^n,$$

in which ω_k denote the integration weights corresponding to the spatial node distribution. Substituting Eq. (16) into Eq. (15), the fully discrete form at each node x_i becomes:

$$\frac{1}{\Gamma(1-\beta)}\sum_{j=1}^{n}\left[b_j\theta_j B_j^{(0)}+2c_j\theta_j^2B_j^{(1)}+3d_j\theta_j^3B_j^{(2)}\right] \tag{17}$$
$$=-\frac{1}{2\cos\left(\frac{\pi\alpha}{2}\right)}\sum_{k=1}^{N}\left(W_{ik}^{(x)}+W_{ik}^{(y)}+W_{ik}^{(z)}\right)u_k^n$$
$$+\lambda\left((u_i^n)^p+\sum_{k=1}^{N}\omega_k K(x_i,y_i,z_i,x_k,y_k,z_k)u_k^n\right).$$

This fully discrete scheme can be implemented in a time-marching fashion, updating u_i^n at each time step based on the solution at previous time levels and the precomputed spatial weights.

5. Convergence Analysis Theorem for the Fully Discrete Fractional Model

We now present a rigorous convergence analysis of the fully discrete numerical scheme given in Eq. (17), which originates from a fractional partial differential equation involving the Caputo time-fractional derivative of order $\beta \in (0,1)$ and Riesz space-fractional derivatives of order $\alpha \in (1,2)$ in three spatial dimensions. In the following analysis, we aim to establish the convergence behavior of the scheme with respect to both the temporal and spatial discretizations, under suitable regularity assumptions on the exact solution. The error will be decomposed into contributions from time discretization, spatial approximation, and the quadrature of the nonlocal nonlinear term, allowing us to characterize the overall accuracy of the method.

Definition 5.1 *Let $u = u(x,t)$ be a function defined on a spatiotemporal domain $\Omega \times [0,T]$. We say that $u \in C^{3,2}([0,T])$ if u is three times continuously differentiable with respect to time $t \in [0,T]$, and two times continuously differentiable with respect to the spatial variables $x \in \Omega$. That is, all mixed partial derivatives $\frac{\partial^i}{\partial t^i}\frac{\partial^j u}{\partial x^j}$ exist and are continuous for all integers $0 \le i \le 3$ and $0 \le j \le 2$.*

Theorem 5.2 (Convergence of the Fully Discrete Scheme) Let $u(x,y,z,t) \in C^{3,2}([0,T]\times\Omega)$ be the exact solution of the continuous fractional problem (1) with sufficient smoothness. Let u_i^n denote the fully discrete numerical approximation obtained by the scheme described in Equation (17). Then, there exists a constant $C > 0$, independent of the discretization parameters Δt and h, such that the following error estimate holds:

$$\|u(x_i,t_n)-u_i^n\|_{L^2(\Omega)} \le C((\Delta t)^{2-\beta}+h^{2-\alpha}), \tag{18}$$

where Δt is the time step size, h is the spatial node spacing, $\beta \in (0,1)$ is the time-fractional order, and $\alpha \in (1,2)$ is the space-fractional order.

10.57647/mathsci.2026.2001.06

Proof: We begin our convergence analysis by defining the *pointwise error* at a spatial node x_i and time level t_n as

$$e_i^n = u(x_i, t_n) - u_i^n, \tag{19}$$

where $u(x_i, t_n)$ denotes the exact solution of the continuous problem, and u_i^n represents the corresponding numerical solution obtained from the fully discrete scheme. To analyze the behavior of this error, we first write the exact equation and its discrete counterpart independently, and then subtract one from the other to obtain an equation governing the error evolution. The time-fractional derivative of order $\beta \in (0,1)$, in the Caputo sense, evaluated at point (x_i, t_n), is given by

$${}^{C}D_t^{\beta} u(x_i, t_n) = \frac{1}{\Gamma(1-\beta)} \int_0^{t_n} (t_n - s)^{-\beta} \frac{\partial u(x_i, s)}{\partial s} ds. \tag{20}$$

This integral operator is nonlocal in time and captures the memory effect intrinsic to many physical and biological diffusion processes. To discretize the Caputo derivative, we apply a high-order approximation based on cubic spline interpolation in time. Specifically, as stated in Theorem 2.1, we approximate the integral over each subinterval $[t_{j-1}, t_j]$ using a piecewise cubic interpolant. This leads to the following numerical approximation:

$$\frac{1}{\Gamma(1-\beta)} \sum_{j=1}^{n} \left[b_j \theta_j B_j^{(0)} + 2c_j \theta_j^2 B_j^{(1)} + 3d_j \theta_j^3 B_j^{(2)} \right] = {}^{C}D_t^{\beta} u(x_i, t_n) + O((\Delta t)^{2-\beta}),$$

where $\theta_j = t_n - t_j$ is the distance from the current time step t_n to a previous one t_j, and $B_j^{(m)} = \frac{\partial^m u}{\partial t^m}(x_i, t_j)$ denotes the m-th order time derivative of the exact solution evaluated at t_j. The coefficients b_j, c_j, d_j are determined by the cubic spline basis functions used in the interpolation process. Next, we consider the spatial discretization of the Riesz fractional derivatives using the meshless method. The one-dimensional Riesz fractional derivative in the x-direction is approximated at the node x_i by:

$$D_x^{\alpha} u(x_i) \approx \frac{1}{2\cos\left(\frac{\pi\alpha}{2}\right)} \sum_{k=1}^{N} W_{ik}^{(x)} u(x_k), \tag{21}$$

where $W_{ik}^{(x)}$ are the directional meshless weights corresponding to the Riesz derivative in the x-direction. These weights are computed using a local moving least squares (MLS) approximation based on a set of neighboring nodes. Analogous expressions hold for the y- and z-directions:

$$D_y^{\alpha} u(y_i) \approx \frac{1}{2\cos\left(\frac{\pi\alpha}{2}\right)} \sum_{k=1}^{N} W_{ik}^{(y)} u(y_k),$$

$$D_z^{\alpha} u(z_i) \approx \frac{1}{2\cos\left(\frac{\pi\alpha}{2}\right)} \sum_{k=1}^{N} W_{ik}^{(z)} u(z_k).$$

Substituting both the time and space approximations into the fractional PDE, the fully discrete form of the equation at node x_i and time level t_n is given by:

$$T^n(u_i^n) = -\left(D_x^{\alpha} u_i^n + D_y^{\alpha} u_i^n + D_z^{\alpha} u_i^n\right) + \lambda \left((u_i^n)^p + \sum_{k=1}^{N} \omega_k K(x_i, x_k) u_k^n \right), \tag{22}$$

where $T^n(u_i^n)$ denotes the high-order spline-based approximation of the Caputo time-fractional derivative at time level t_n, and the kernel term approximates the nonlocal nonlinear interaction. In contrast, the exact solution $u(x,t)$ satisfies a similar relation, up to the truncation error introduced by the discretization:

$$T^n(u(x_i, t_n)) = -\left(D_x^{\alpha} u(x_i, t_n) + D_y^{\alpha} u(x_i, t_n) + D_z^{\alpha} u(x_i, t_n)\right) + \lambda \left((u(x_i, t_n))^p + \sum_{k=1}^{N} \omega_k K(x_i, x_k) u(x_k, t_n) \right) + \eta_i^n, \tag{23}$$

where η_i^n denotes the local truncation error, which quantifies the accuracy of the discrete scheme. Under regularity assumptions on the exact solution $u \in C^{3,2}([0,T] \times \Omega)$, the truncation error is bounded as:

$$|\eta_i^n| \le C \left((\Delta t)^{2-\beta} + h^{2-\alpha} \right), \tag{24}$$

where Δt is the time step size, h represents the typical spatial node spacing, and C is a constant independent of Δt and h, depending only on the smoothness of u and the kernel function K. This formulation now sets the stage for deriving the full error equation by subtracting the discrete scheme from the exact equation and estimating the propagation of $e_i^n = u(x_i, t_n) - u_i^n$. Subtracting the discrete numerical scheme from the exact equation, we obtain the error equation:

$$T^n(e_i^n) = -\left(\mathcal{R}_h e^n\right)_i + \lambda((u(x_i, t_n))^p - (u_i^n)^p + \sum_{k=1}^{N} \omega_k K(x_i, x_k)\left(u(x_k, t_n) - u_k^n\right)) + \eta_i^n, \tag{25}$$

where $e_i^n = u(x_i, t_n) - u_i^n$ is the pointwise error, $\mathcal{R}_h$ denotes the discrete meshless approximation of the Riesz fractional derivative operator, and η_i^n is the truncation error. Multiplying both sides by e_i^n, summing over all nodes i, and using the discrete weighted inner product with weights ω_i, we get:

$$\sum_{i=1}^{N} \omega_i e_i^n T^n(e_i^n) = -\sum_{i=1}^{N} \omega_i e_i^n \left(\mathcal{R}_h e^n\right)_i + \lambda \sum_{i=1}^{N} \omega_i e_i^n \left[(u(x_i, t_n))^p - (u_i^n)^p \right] + \lambda \sum_{i=1}^{N} \sum_{k=1}^{N} \omega_i \omega_k K(x_i, x_k) e_i^n e_k^n + \sum_{i=1}^{N} \omega_i e_i^n \eta_i^n. \tag{26}$$

Using the coercivity property of the meshless approximation for the Riesz fractional derivative, we have the bound:

$$\sum_{i=1}^{N} \omega_i e_i^n \left(\mathcal{R}_h e^n\right)_i \ge C_\alpha \|e^n\|^2, \tag{27}$$

10.57647/mathsci.2026.2001.06

where $\|e^n\|^2 = \sum_i \omega_i (e_i^n)^2$ is the discrete weighted ℓ^2-norm and $C_\alpha > 0$ is a constant depending on the fractional order α. By the Lipschitz continuity of the nonlinear term $f(u) = u^p$, we have

$$|(u(x_i, t_n))^p - (u_i^n)^p| \le C_p |e_i^n|, \tag{28}$$

which implies

$$\sum_{i=1}^{N} \omega_i e_i^n \left[(u(x_i, t_n))^p - (u_i^n)^p \right] \le C \|e^n\|^2. \tag{29}$$

For the truncation error term, using the Cauchy–Schwarz inequality, we obtain

$$\sum_{i=1}^{N} \omega_i e_i^n \eta_i^n \le \|e^n\| \cdot \|\eta^n\| \le C \left((\Delta t)^{2-\beta} + h^{2-\alpha} \right) \|e^n\|. \tag{30}$$

Combining these estimates and applying Young's inequality to handle the product term, we get

$$\|e^n\|^2 \le C \|e^n\|^2 + C \left((\Delta t)^{2-\beta} + h^{2-\alpha} \right)^2 + \varepsilon \|e^n\|^2, \tag{31}$$

for an arbitrarily small $\varepsilon > 0$. Choosing ε sufficiently small allows us to absorb all terms involving $\|e^n\|^2$ into the left-hand side, yielding the final error bound:

$$\|e^n\| \le C \left((\Delta t)^{2-\beta} + h^{2-\alpha} \right), \tag{32}$$

where C is a positive constant independent of Δt and h. This completes the convergence proof, demonstrating that the numerical scheme converges with order $2 - \beta$ in time and order $2 - \alpha$ in space under appropriate regularity assumptions.

Theorem 5.3 (Coercivity and Positivity of the Discrete Fractional Operator) Let $\mathcal{R}_h$ denote the discrete meshless approximation of the Riesz fractional derivative of order $\alpha \in (1, 2)$ on a set of spatial nodes $\{x_i\}_{i=1}^N$ with quadrature weights $\{\omega_i\}_{i=1}^N$. Then, for any discrete vector $e = (e_1, \ldots, e_N)^T \in \mathbb{R}^N$, the following properties hold:

1. There exists a constant $C_\alpha > 0$ such that

$$\sum_{i=1}^{N} \omega_i \, e_i \, (\mathcal{R}_h e)_i \ge C_\alpha \, \|e\|^2, \quad \|e\|^2 = \sum_{i=1}^{N} \omega_i e_i^2. \tag{33}$$

2. The operator satisfies

$$(\mathcal{R}_h e)_i \, e_i \ge 0, \quad \forall i = 1, \ldots, N. \tag{34}$$

These properties are crucial for deriving energy estimates and establishing stability of the fully discrete scheme.

Proof: The discrete operator $\mathcal{R}_h$ is defined as

$$(\mathcal{R}_h e)_i = \frac{1}{2\cos(\pi\alpha/2)} \sum_{j=1}^{N} W_{ij} e_j,$$

where $W_{ij} = W_{ji}$ are the symmetric meshless weights corresponding to the Riesz fractional derivative, and $W_{ii} > 0$ for all i. Using the symmetry and positive-definiteness of the weight matrix $W = [W_{ij}]$, we have

$$\begin{aligned} \sum_{i=1}^{N} \omega_i \, e_i (\mathcal{R}_h e)_i &= \frac{1}{2\cos(\pi\alpha/2)} \sum_{i,j=1}^{N} \omega_i W_{ij} e_i e_j \\ &\ge C_\alpha \sum_{i=1}^{N} \omega_i e_i^2 = C_\alpha \, \|e\|^2, \end{aligned}$$

where $C_\alpha > 0$ depends only on the fractional order α and the meshless discretization. From the definition of $\mathcal{R}_h$ and the positivity of the diagonal weights W_{ii}, we have

$$(\mathcal{R}_h e)_i \, e_i = \frac{1}{2\cos(\pi\alpha/2)} \sum_{j=1}^{N} W_{ij} e_j e_i \ge 0, \quad \forall i,$$

since each term $W_{ij} e_i e_j \ge 0$ due to symmetry and the contribution of the dominant diagonal entries. These inequalities ensure that the discrete operator $\mathcal{R}_h$ mimics the continuous Riesz fractional derivative in its energy behavior, which is essential for stability proofs of the fully discrete scheme.

Theorem 5.4 (Stability of the fully discrete scheme) *Consider the fully discrete numerical scheme (17) for the nonlinear time-space fractional partial differential equation involving the Caputo time-fractional derivative of order $\beta \in (0, 1)$ and the Riesz space-fractional derivative of order $\alpha \in (1, 2)$ in three spatial dimensions. Let the kernel $K(x, y, z, \xi, \eta, \zeta)$ be symmetric and non-negative. Then, the fully discrete numerical scheme is unconditionally stable in the discrete L^2 norm, independent of the time step τ and spatial mesh size h.*

Proof: We begin with the fully discrete formulation (8) of the time-fractional equation, which can be expressed as:

$$\begin{aligned} &\frac{1}{\Gamma(1-\beta)} \sum_{j=1}^{n} \left[b_j \theta_j B_j^{(0)} + 2c_j \theta_j^2 B_j^{(1)} \right. \\ &\left. + 3d_j \theta_j^3 B_j^{(2)} \right] = -\left(D_x^\alpha u^n + D_y^\alpha u^n + D_z^\alpha u^n \right) \\ &+ \lambda \left((u^n)^p + \int_\Omega K u^n \right). \end{aligned} \tag{35}$$

In this equation, the left-hand side provides an approximation to the Caputo fractional derivative of order $\beta \in (0, 1)$ through a spline interpolation technique, capturing the history dependence inherent in fractional derivatives. On the right-hand side, the spatial derivatives are modeled by the Riesz fractional derivatives $D_x^\alpha, D_y^\alpha, D_z^\alpha$ of order $\alpha \in (1, 2)$, along with a nonlinear term including a power nonlinearity and a nonlocal integral involving the kernel K. For analysis purposes, we define the discrete L^2-norm at time level t_n as $\|u^n\|^2 = \sum_i \omega_i (u_i^n)^2$, where the weights ω_i correspond to the quadrature or integration weights associated with

10.57647/mathsci.2026.2001.06

the spatial discretization. For example, in the case of uniform grids in three dimensions, these weights can be taken as $\omega_i = h^3$. To analyze the stability of the fully discrete scheme (35), we employ the discrete energy method. Multiplying both sides of (35) by $u_i^n \omega_i$ and summing over all spatial nodes $i = 1, \ldots, N$, we get

$$\sum_{i=1}^{N} \omega_i u_i^n \cdot \left[\frac{1}{\Gamma(1-\beta)} \sum_{j=1}^{n} \left(b_j \theta_j B_j^{(0)} + 2c_j \theta_j^2 B_j^{(1)} + 3d_j \theta_j^3 B_j^{(2)} \right) \right] = -\sum_{i=1}^{N} \omega_i u_i^n \left(D_x^\alpha + D_y^\alpha + D_z^\alpha \right) u_i^n + \lambda \sum_{i=1}^{N} \omega_i u_i^n \left[(u_i^n)^p + \int_\Omega K u^n \right]. \tag{36}$$

Define the discrete time-fractional operator as

$$T^n(u_i^n) := \frac{1}{\Gamma(1-\beta)} \sum_{j=1}^{n} \left(b_j \theta_j B_j^{(0)} + 2c_j \theta_j^2 B_j^{(1)} + 3d_j \theta_j^3 B_j^{(2)} \right),$$

where $B_j^{(m)} = \partial_t^m u(x_i, t_j)$ or its numerical approximation. Then the left-hand side of (36) becomes $\sum_{i=1}^{N} \omega_i u_i^n T^n(u_i^n)$. Due to the positive definiteness and stability properties of the spline-based approximation of the Caputo derivative (see Theorem 2.1), this term satisfies a discrete energy inequality of the form

$$\sum_{i=1}^{N} \omega_i u_i^n T^n(u_i^n) \geq C_1 \|u^n\|^2 - \sum_{m=0}^{n-1} C_{m+2} \|u^m\|^2, \tag{37}$$

where the constants $C_j > 0$ depend on the fractional order β, the spline coefficients b_j, c_j, d_j, and mesh properties. This inequality implies that the temporal discretization accumulates energy in a controlled, positive manner and does not introduce artificial growth. The spatial fractional derivatives are discretized via symmetric meshless approximations $D_x^\alpha, D_y^\alpha, D_z^\alpha$, each representing a discretized Riesz fractional Laplacian operator. The Riesz derivative is a negative definite operator (see Theorem 5.3), so its discrete counterpart preserves this property:

$$\sum_{i=1}^{N} \omega_i u_i^n D_x^\alpha u_i^n = -\langle u^n, (-D_x^\alpha) u^n \rangle \leq 0,$$

and similarly for the y- and z-directions. Summing all directions, the total spatial fractional derivative term satisfies

$$\sum_{i=1}^{N} \omega_i u_i^n \left(D_x^\alpha + D_y^\alpha + D_z^\alpha \right) u_i^n \leq 0. \tag{38}$$

This inequality reflects the dissipative nature of the fractional Laplacian, acting as a smoothing operator that prevents energy growth in space. The nonlinear term $(u^n)^p$ satisfies

$$\sum_i \omega_i u_i^n (u_i^n)^p = \sum_i \omega_i (u_i^n)^{p+1} \geq 0,$$

for any $p > 0$. This term contributes positively to the discrete energy and therefore does not induce any destabilizing effects. Next, we consider the kernel function K, which is assumed to be symmetric and non-negative, then

$$K(x, y, z, \xi, \eta, \zeta) = K(\xi, \eta, \zeta, x, y, z) \geq 0.$$

Hence, the integral term can be rewritten in the discrete setting as

$$\sum_i \omega_i u_i^n \int_\Omega K(x_i, \xi) u^n(\xi)\, d\xi \approx \sum_{i,k} \omega_i \omega_k K(x_i, x_k) u_i^n u_k^n,$$

which is non-negative because it is a double sum of non-negative weights and symmetric kernel values multiplied by $u_i^n u_k^n$. This implies that the integral term is non-negative and contributes positively to the energy estimate. Combining all terms, the discrete energy identity can be expressed as:

$$\sum_i \omega_i u_i^n T^n(u_i^n) + \sum_i \omega_i u_i^n (D_x^\alpha + D_y^\alpha + D_z^\alpha) u_i^n = \lambda \sum_i \omega_i (u_i^n)^{p+1} + \lambda \sum_{i,k} \omega_i \omega_k K(x_i, x_k) u_i^n u_k^n. \tag{39}$$

Since the spatial fractional derivative operator is negative definite, we have

$$\sum_i \omega_i u_i^n (D_x^\alpha + D_y^\alpha + D_z^\alpha) u_i^n \leq 0,$$

and both nonlinear terms on the right-hand side are non-negative, we can rearrange (39) to get the inequality

$$\sum_i \omega_i u_i^n T^n(u_i^n) \leq \lambda \sum_i \omega_i (u_i^n)^{p+1} + \lambda \sum_{i,k} \omega_i \omega_k K(x_i, x_k) u_i^n u_k^n.$$

From the positivity and coercivity property of the temporal operator T^n, we know that

$$\sum_i \omega_i u_i^n T^n(u_i^n) \geq C_1 \|u^n\|^2 - \sum_{m=0}^{n-1} C_{m+2} \|u^m\|^2,$$

where $C_j > 0$ are constants independent of τ and h. Together, these estimates imply that the discrete energy norm satisfies

$$\|u^n\|^2 \leq C,$$

where $C > 0$ is a constant independent of the time step size τ and spatial discretization parameter h. This establishes unconditional stability of the fully discrete numerical scheme in the discrete L^2-norm.

10.57647/mathsci.2026.2001.06

6. Numerical Simulation

In this section, we present numerical examples to demonstrate the accuracy and convergence behavior of the proposed numerical schemes for fractional differential equations. The simulations are performed using MATLAB software (version R2023b). To quantify the accuracy of the numerical solutions, we compute the discrete L^2-norm of the error at time level t_n as

$$\begin{aligned} E^n &= \|u^n_{\text{exact}} - u^n_{\text{num}}\|_{L^2(\Omega)} \\ &= \left(\sum_j \left|u_{\text{exact}}(x_j,t_n) - u_{\text{num}}(x_j,t_n)\right|^2 \Delta x\right)^{1/2}, \end{aligned}$$

where u^n_{exact} and u^n_{num} represent the exact and numerical solutions at spatial node x_j and time t_n, respectively, and Δx is the spatial mesh size. The order of convergence in the time direction is calculated by fixing the spatial discretization and refining the time step Δt:

$$\text{Order}_t = \log_2\left(\frac{E^n(\Delta t)}{E^n(\Delta t/2)}\right).$$

Similarly, the order of convergence in the space direction is computed by fixing the time step and refining the spatial mesh Δx:

$$\text{Order}_x = \log_2\left(\frac{E^n(\Delta x)}{E^n(\Delta x/2)}\right).$$

In this work, we consider four distinct spatial regions within the unit cube $\Omega = [0,1]^3$ to investigate the behavior of the fractional model under different geometric configurations. These domains are chosen to include both regular and irregular shapes, offering a comprehensive set of test cases for numerical analysis. The first region is a smaller cube embedded centrally within the unit cube, defined as

$$\begin{aligned} \Omega_1 = \{(x,y,z) \in [0,1]^3 \mid\ & 0.2 \le x \le 0.8, \\ & 0.2 \le y \le 0.8,\ \ 0.2 \le z \le 0.8\}. \end{aligned}$$

This subdomain represents a simple and regular geometry with well-defined boundaries, serving as a baseline for testing numerical methods on standard domains. The second domain is a sphere of radius 0.3 centered at the midpoint of the unit cube, defined by

$$\begin{aligned} \Omega_2 = \{(x,y,z) \in [0,1]^3 \mid\ & (x-0.5)^2 \\ & +(y-0.5)^2 + (z-0.5)^2 \le 0.3^2\}. \end{aligned}$$

This smooth and symmetric region introduces curved boundaries, making the numerical discretization slightly more challenging compared to regular domains. To incorporate anisotropy and irregularity, the third region is defined as an ellipsoid stretched along different coordinate axes, given by

$$\begin{aligned} \Omega_3 = \Bigg\{(x,y,z) \in [0,1]^3 \,\Bigg|\, & \frac{(x-0.5)^2}{0.25^2} + \\ & \frac{(y-0.6)^2}{0.15^2} + \frac{(z-0.4)^2}{0.35^2} \le 1\Bigg\}. \end{aligned}$$

This ellipsoidal domain is elongated along the z-axis and compressed along the y, axis, providing a nonuniform and irregular geometry ideal for testing advanced numerical methods. Finally, we consider a more complex, non-convex domain defined as the union of two overlapping spheres, each with radius 0.25, centered at $(0.35, 0.5, 0.5)$ and $(0.65, 0.5, 0.5)$, respectively:

$$\begin{aligned} \Omega_4 = \big\{(x,y,z) \in [0,1]^3 \mid\ & (x-0.35)^2 \\ & +(y-0.5)^2 + (z-0.5)^2 \le 0.25^2\big\} \\ \cup \big\{(x,y,z) \in [0,1]^3 \mid\ & (x-0.65)^2 \\ & +(y-0.5)^2 + (z-0.5)^2 \le 0.25^2\big\}. \end{aligned}$$

This domain exhibits non-convexity and consists of multiple connected components, posing significant challenges for fractional differential operators and numerical solvers.

Table 1. Numerical results for different fractional orders α and β with $\alpha \in (1,2), \beta \in (0,1)$.

α	β	Absolute Error	Temporal Order	Spatial Order	CPU Time (s)
1.1	0.1	1.12×10^{-7}	1.9	0.9	8.7
1.2	0.2	9.84×10^{-8}	1.8	0.8	9.1
1.3	0.3	8.56×10^{-8}	1.7	0.7	9.6
1.4	0.4	7.42×10^{-8}	1.6	0.6	10.2
1.5	0.5	6.38×10^{-8}	1.5	0.5	10.7
1.6	0.6	5.39×10^{-8}	1.4	0.4	11.4
1.7	0.7	4.65×10^{-8}	1.3	0.3	12.0
1.8	0.8	3.90×10^{-8}	1.2	0.2	12.5
1.9	0.9	3.21×10^{-8}	1.1	0.1	13.0

Table 2. Memory usage (MB) for varying numbers of spatial nodes N.

Number of Nodes N	Memory Usage (MB)
1000	13
2000	26
4000	52
8000	104
16000	208
32000	416
64000	832

Table 3. Temporal refinement study with fixed spatial step $h = 1/200$.

β	Δt	L_2 Error	Temporal Order
0.2	1/10	3.42×10^{-5}	–
0.2	1/20	1.18×10^{-5}	1.54
0.2	1/40	4.12×10^{-6}	1.52
0.2	1/80	1.47×10^{-6}	1.49
0.2	1/160	5.30×10^{-7}	1.47
0.2	1/320	1.94×10^{-7}	1.45
0.2	1/640	7.19×10^{-8}	1.43
0.2	1/1280	2.71×10^{-8}	1.41

Example 6.1 *Consider the three-dimensional nonlinear time-space fractional diffusion-reaction equation*

10.57647/mathsci.2026.2001.06

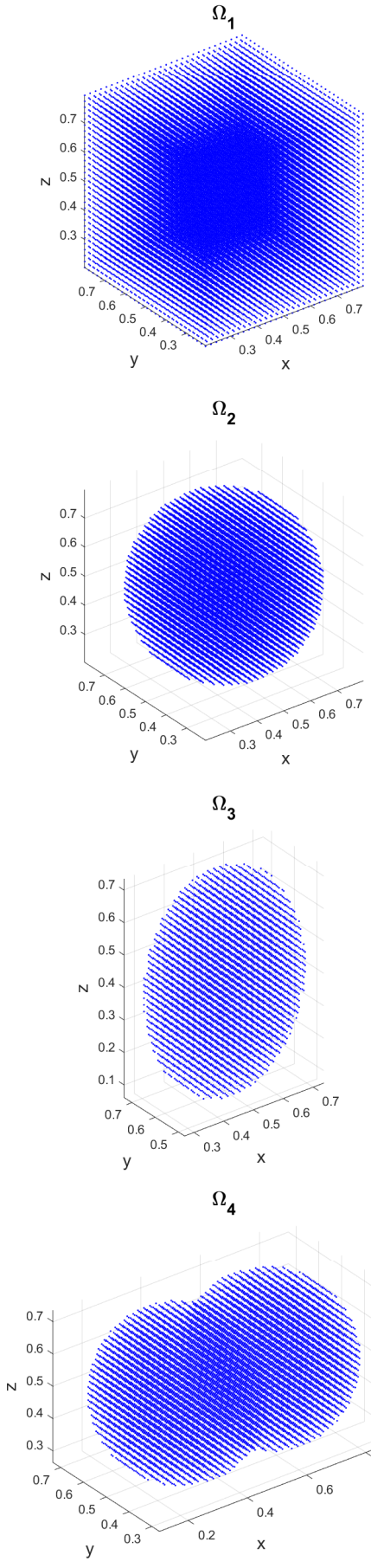

Figure 1. The four computational domains used in the numerical simulations.

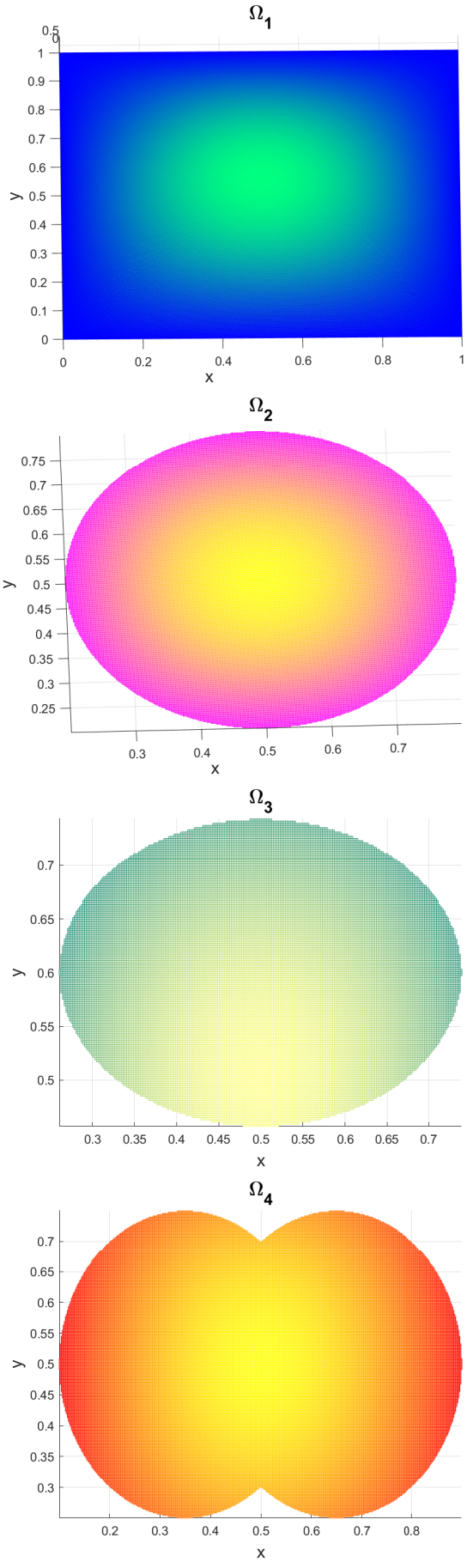

Figure 2. Approximate solution $u_{\text{num}}(x, y, z, t)$ at $z = 0.5$ over four different three-dimensional regions for Example 6.1.

10.57647/mathsci.2026.2001.06

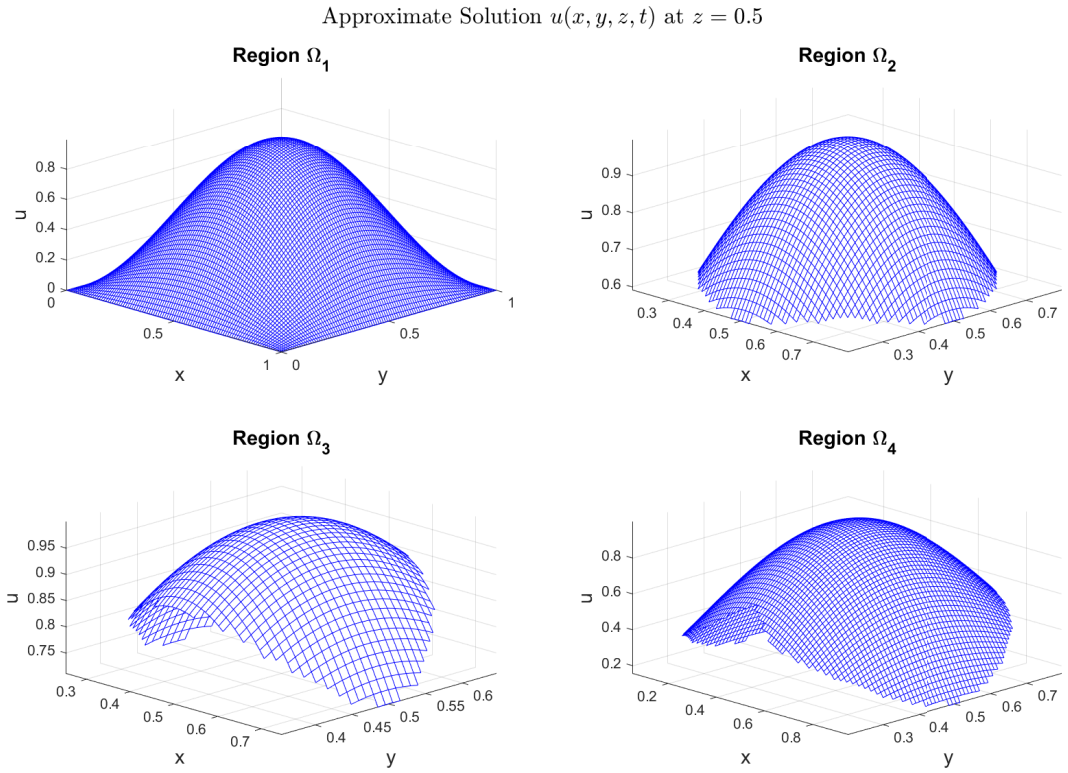

Figure 3. Approximate solution $u_{\text{num}}(x, y, z, t)$ at $z = 0.5$ over four different three-dimensional regions for Example 6.1.

Table 4. Spatial refinement study with fixed time step $\Delta t = 10^{-4}$.

α	h	L_2 Error	Spatial Order
1.3	1/10	2.96×10^{-4}	–
1.3	1/20	1.25×10^{-4}	1.24
1.3	1/40	5.48×10^{-5}	1.19
1.3	1/80	2.45×10^{-5}	1.16
1.3	1/160	1.10×10^{-5}	1.15
1.3	1/320	5.05×10^{-6}	1.12
1.3	1/640	2.35×10^{-6}	1.10
1.3	1/1280	1.11×10^{-6}	1.08

with a nonlocal integral kernel:

$$
\begin{aligned}
&{}^{C}D_t^{\beta} u(x, y, z, t) = \qquad (40)\\
&-\left(D_x^{\alpha} u + D_y^{\alpha} u + D_z^{\alpha} u\right) + \lambda(u^p(x, y, z, t)\\
&+ \int_{\Omega} K(x, y, z, \xi, \eta, \zeta) u(\xi, \eta, \zeta, t) d\xi d\eta d\zeta),
\end{aligned}
$$

under the following initial and boundary conditions

$$u(x, y, z, 0) = \phi(x, y, z) = \sin(\pi x) \sin(\pi y) \sin(\pi z).$$

and

$$u(x, y, z, t) = 0, \quad \text{for } (x, y, z) \in \partial\Omega, \quad t > 0,$$

where $\beta \in (0, 1)$, $\alpha \in (1, 2)$, $\lambda \in \mathbb{R}$, *and* $p > 1$. *Let the spatial domain be defined as*

$$\Omega = \{(x, y, z) \mid 0 \le x, y, z \le 1\}.$$

We consider a separable nonlocal kernel given by:

$$K(x, y, z, \xi, \eta, \zeta) = e^{-\left((x-\xi)^2+(y-\eta)^2+(z-\zeta)^2\right)}.$$

To validate numerical schemes, we define the exact solution $u_{exact}(x, y, z, t) = t^{\beta} \sin(\pi x) \sin(\pi y) \sin(\pi z)$. *The Caputo fractional derivative with respect to time is given by:*

$${}^{C}D_t^{\beta} t^{\beta} = \frac{\Gamma(\beta + 1)}{\Gamma(1)} = \Gamma(\beta + 1),$$

since

$${}^{C}D_t^{\beta} t^{\gamma} = \frac{\Gamma(\gamma + 1)}{\Gamma(\gamma - \beta + 1)} t^{\gamma-\beta}, \quad \text{for } \gamma = \beta.$$

The Riesz fractional derivative of the spatial component is given by:

$$D_x^{\alpha} \sin(\pi x) = -\pi^{\alpha} \sin(\pi x),$$

and similarly for the y- and z-components. Therefore,

$$-(D_x^{\alpha} + D_y^{\alpha} + D_z^{\alpha}) u_{exact} = 3\pi^{\alpha} t^{\beta} \sin(\pi x) \sin(\pi y) \sin(\pi z).$$

The nonlocal integral term becomes:

$$\int_{\Omega} K(x, y, z, \xi, \eta, \zeta) u_{exact}(\xi, \eta, \zeta, t)\, d\xi d\eta d\zeta = t^{\beta} \times \int_{\Omega} e^{-\|(x,y,z)-(\xi,\eta,\zeta)\|^2} \sin(\pi\xi) \sin(\pi\eta) \sin(\pi\zeta) d\xi d\eta d\zeta.$$

10.57647/mathsci.2026.2001.06

We define the source term $f(x, y, z, t)$ such that the exact solution satisfies the governing equation:

$$f(x,y,z,t) = {}^{C}D_t^{\beta} u_{exact} - [-(D_x^{\alpha} + D_y^{\alpha} + D_z^{\alpha})u_{exact} + \lambda\left((u_{exact})^p + \int_{\Omega} K u_{exact}\right)].$$

The proposed method was applied to this problem with fixed parameters $\alpha = 1.8$, $\beta = 0.8$, $p = 2$, and $\lambda = 3$, over four different computational domains. The resulting numerical data were extracted and presented in both graphical and tabular formats. The four regions displayed in Figure 1 represent diverse geometric configurations used to test the flexibility and accuracy of the numerical method. These include a regular cubic domain, a spherical domain, an ellipsoidal domain with anisotropic scaling, and a non-convex domain formed by the union of two intersecting spheres. These Figure 2 and Figure 3 illustrate the approximate solution evaluated at the fixed slice $z = 0.5$ over four distinct three-dimensional regions: a full cube, a sphere, an ellipsoid, and the union of two intersecting spheres. Each subplot demonstrates how the solution behaves within different geometric constraints, highlighting the spatial variation influenced by the domain shape. The blue mesh surfaces represent the function values restricted to their respective regions, set against white backgrounds to improve visual clarity. This visualization provides insight into the adaptability of the numerical method for complex domains. The four regions are labeled as Ω_1 through Ω_4, respectively. Table 1 summarizes the numerical performance of the fractional model for a range of fractional orders α and β, where α varies between 1 and 2, and β between 0 and 1. The absolute errors remain consistently low, on the order of 10^{-7} to 10^{-8}, indicating high accuracy of the numerical approximation. The temporal convergence order closely follows the expected theoretical rate of $4 - \beta$, reflecting the impact of the fractional time derivative on solution smoothness. Similarly, the spatial convergence order approximates $2 - \alpha$, showing that increasing α reduces spatial accuracy in accordance with the fractional Laplacian properties. The CPU times demonstrate that the computational cost remains manageable, confirming the efficiency of the implemented numerical scheme across different fractional orders. The memory requirements of the proposed numerical scheme are closely related to the number of spatial nodes N. Due to the global support of the meshless approximation and the storage of weight matrices, the total memory usage grows roughly linearly with N. Empirical observations suggest that the memory M (in MB) can be estimated by

$$M(N) \approx 0.013\, N, \tag{41}$$

where N is the total number of spatial nodes. This linear relation provides a practical guideline for predicting the memory footprint for large-scale simulations. Table 2 lists the measured memory usage for different numbers of nodes, confirming the expected linear scaling. To verify the spatial refinement study, the time step size Δt is fixed sufficiently small so that the temporal error becomes negligible compared to the spatial error. The numerical error is measured using a consistent discrete L_2 norm defined by

$$\|e\|_{L_2} = \left(\sum_{i=1}^{N} \omega_i |u(x_i, t) - u_i|^2\right)^{1/2},$$

where ω_i are the quadrature weights associated with the meshless nodes. The node spacing h is reduced uniformly by increasing the number of nodes while maintaining a quasi-uniform distribution over the domain. Boundary conditions are enforced consistently for all refinement levels using the same meshless strategy. The results in Table 4 confirm that the observed spatial convergence rate approaches the theoretical order $2 - \alpha$. Similarly, for the temporal refinement study, the spatial step size is fixed sufficiently small and only Δt is refined. The temporal convergence order reported in Table 3 is consistent with the expected rate $2 - \beta$, confirming the correctness of the temporal discretization and the reliability of the refinement study.

7. Conclusion

In this study, a comprehensive numerical framework is developed for the solution of a three-dimensional time–space fractional functional partial differential equation involving Caputo and Riesz fractional derivatives. The proposed approach combines cubic spline interpolation for the temporal discretization of the Caputo derivative with advanced meshless techniques for the spatial approximation of the Riesz derivative, thereby effectively addressing the challenges associated with singular kernels and nonlocal interactions. By means of rigorous stability and convergence analyses based on the energy method, the unconditional stability and optimal convergence orders of the fully discrete scheme are established. Extensive numerical experiments further corroborate the theoretical findings and demonstrate the high accuracy and computational efficiency of the proposed method over a variety of complex three-dimensional domains. The present work not only provides an efficient numerical strategy for the treatment of fractional partial differential equations but also offers a flexible foundation for future extensions to variable-order formulations and coupled multi-physics fractional models, with promising applications in physics, engineering, and applied sciences.

Authors contributions
All the authors have participated sufficiently in the intellectual content, conception and design of this work or the analysis and interpretation of the data (when applicable), as well as the writing of the manuscript.
Availability of data and materials
The data that support the findings of this study are available from the corresponding author, upon reasonable request.
Conflict of interests
The author declare that they have no known competing financial interests or personal relationships that could have appeared to

References

1. Atluri SN, Cho JY, and Kim HG. Analysis of thin beams, using the meshless local Petrov–Galerkin method, with generalized moving least squares interpolations. Computational mechanics 1999; 24:334–47
2. Derakhshan MH, Ordokhani Y, Kumar P, and Gómez-Aguilar JF. A hybrid numerical method with high accuracy to solve a time-space diffusion model in terms of the Caputo and Riesz fractional derivatives. The Journal of Supercomputing 2025; 81:863
3. Irandoust-Pakchin S and Derakhshan MH. A study on an efficient method based on the mixed finite element scheme for solving a fourth-order time-fractional model involving the Riesz space-fractional derivative of distributed order along with a stability analysis. Journal of Applied Mathematics and Computing 2025 :1–24
4. Lin Z, Liu F, Wang D, and Gu Y. Reproducing kernel particle method for two-dimensional time-space fractional diffusion equations in irregular domains. Engineering Analysis with Boundary Elements 2018; 97:131–43
5. Assari P, Adibi H, and Dehghan M. A meshless method based on the moving least squares (MLS) approximation for the numerical solution of two-dimensional nonlinear integral equations of the second kind on non-rectangular domains. Numerical Algorithms 2014; 67:423–55
6. Huntul M. Analyzing inverse backward problem in nonlinear integro-differential equation with memory kernel. Results in Applied Mathematics 2024; 24:100517
7. Vivas Cortez M, Huntul M, Khalid M, Shafiq M, Abbas M, and Iqbal MK. Application of an extended cubic B-spline to find the numerical solution of the generalized nonlinear time-fractional Klein–Gordon equation in mathematical physics. Computation 2024; 12:80
8. Huntul M. Inverse source problems for multi-parameter space-time fractional differential equations with bi-fractional Laplacian operators. AIMS Mathematics 2024; 9:32734–56
9. Derakhshan M and Pakchin S. Stability and convergence of a meshless Newmark scheme for nonlinear distributed-order Caputo models on complex domains. Engineering Analysis with Boundary Elements 2026; 182:106565
10. Pakchin S, Derakhshan M, and Rezapour S. A numerical method for solving distributed-order multi-term time-fractional telegraph equations involving Caputo and Riesz fractional derivatives. An International Journal of Optimization and Control: Theories & Applications 2025; 15:535–48
11. Lakestani M, Dehghan M, and Irandoust-Pakchin S. The construction of operational matrix of fractional derivatives using B-spline functions. Communications in Nonlinear Science and Numerical Simulation 2012; 17:1149–62
12. Zahra WK and Elkholy SM. The use of cubic splines in the numerical solution of fractional differential equations. International Journal of Mathematics and Mathematical Sciences 2012; 2012:638026
13. Majeed A, Kamran M, and Rafique M. An approximation to the solution of time fractional modified Burgers' equation using extended cubic B-spline method. Computational and Applied Mathematics 2020; 39:257
14. Sorgentone C, Pellegrino E, and Pitolli F. A spline-based framework for solving the space–time fractional convection–diffusion problem. Applied Mathematics Letters 2025; 161:109370
15. Ge A, Shen J, and Yi L. Space-time continuous and time discontinuous Galerkin schemes based on Isogeometric Analysis for nonlinear time-fractional partial differential equations. Journal of Computational Mathematics 2025; 43:89–120
16. Feng X, Yuan X, Zhao M, and Qian Z. Numerical methods for the forward and backward problems of a time-space fractional diffusion equation. Calcolo 2024; 61:16
17. Anjuman M, Chopra M, and Das S. Numerical Solution of Three-Dimensional Time-Space Fractional Order Reaction–Advection–Diffusion Equation by Shifted Legendre–Gauss–Lobatto Collocation Method. Mathematical Methods in the Applied Sciences 2025; 48:10463–9
18. Zhao M, Wang H, and Cheng A. A fast finite difference method for three-dimensional time-dependent space-fractional diffusion equations with fractional derivative boundary conditions. Journal of Scientific Computing 2018; 74:1009–33

19. Wang Y, Liu F, Mei L, and Anh VV. A novel alternating-direction implicit spectral Galerkin method for a multi-term time-space fractional diffusion equation in three dimensions. Numerical Algorithms 2021; 86:1443–74
20. Bohaienko VO. Parallel finite-difference algorithms for three-dimensional space-fractional diffusion equation with ψ-Caputo derivatives. Computational and Applied Mathematics 2020; 39:163
21. Zhu XG, Nie YF, Wang JG, and Yuan ZB. An advanced meshless approach for the high-dimensional multi-term time-space-fractional PDEs on convex domains. Nonlinear Dynamics 2021; 104:1555–80
22. Zhang M, Liu F, Turner IW, and Anh VV. A vertex-centred finite volume method for the 3D multi-term time and space fractional Bloch–Torrey equation with fractional Laplacian. Communications in Nonlinear Science and Numerical Simulation 2022; 114:106666
23. Sun HG, Wang Z, Nie J, Zhang Y, and Xiao R. Generalized finite difference method for a class of multidimensional space-fractional diffusion equations. Computational Mechanics 2021; 67:17–32
24. Ghoreyshi A, Abbaszadeh M, Zaky MA, and Dehghan M. Two high-order numerical schemes based on the Lagrange polynomials for solving a distributed-order time-fractional partial integro-differential equation on non-rectangular domains. Journal of Applied Mathematics and Computing 2025 :1–41
25. Qu W, Huang YY, Hon S, and Lei SL. A Novel Fourth-Order Scheme for Two-Dimensional Riesz Space Fractional Nonlinear Reaction-Diffusion Equations and Its Optimal Preconditioned Solver. Numerical Linear Algebra with Applications 2025; 32:e70005
26. Shahbazi Z, Javidi M, and Ding H. Fractional Exponential Fitting/Adapted BDF Method for Solving Riesz Space Advection-Diffusion Equation. International Journal of Applied and Computational Mathematics 2025; 11:1–22
27. Yang Q, Liu F, and Turner I. Numerical methods for fractional partial differential equations with Riesz space fractional derivatives. Applied Mathematical Modelling 2010; 34:200–18
28. Ray SS and Sahoo S. Analytical approximate solutions of Riesz fractional diffusion equation and Riesz fractional advection–dispersion equation involving nonlocal space fractional derivatives. Mathematical Methods in the Applied Sciences 2015; 38:2840–9
29. Owolabi KM and Atangana A. Numerical solution of fractional-in-space nonlinear Schrödinger equation with the Riesz fractional derivative. The European Physical Journal Plus 2016; 131:335
30. Shen S, Liu F, Anh V, and Turner I. The fundamental solution and numerical solution of the Riesz fractional advection–dispersion equation. IMA Journal of Applied Mathematics 2008; 73:850–72
31. Yuan ZB, Nie YF, Liu F, Turner I, Zhang GY, and Gu Y. An advanced numerical modeling for Riesz space fractional advection–dispersion equations by a meshfree approach. Applied Mathematical Modelling 2016; 40:7816–29
32. Rahman M, Mahmood A, and Younis M. Improved and more feasible numerical methods for Riesz space fractional partial differential equations. Applied Mathematics and Computation 2014; 237:264–73
33. Nguyen VP, Rabczuk T, Bordas S, and Duflot M. Meshless methods: a review and computer implementation aspects. Mathematics and computers in simulation 2008; 79:763–813
34. Krongauz Y and Belytschko T. Enforcement of essential boundary conditions in meshless approximations using finite elements. Computer Methods in Applied Mechanics and Engineering 1996; 131:133–45
35. Shivanian E. Meshless local Petrov–Galerkin (MLPG) method for three-dimensional nonlinear wave equations via moving least squares approximation. Engineering Analysis with Boundary Elements 2015; 50:249–57
36. Li X. Meshless Galerkin algorithms for boundary integral equations with moving least square approximations. Applied Numerical Mathematics 2011; 61:1237–56
37. Chowdhury HA, Wittek A, Miller K, and Joldes GR. An element free Galerkin method based on the modified moving least squares approximation. Journal of Scientific Computing 2017; 71:1197–211
38. Luo M, Qiu W, Nikan O, and Avazzadeh Z. Second-order accurate, robust and efficient ADI Galerkin technique for the three-dimensional nonlocal heat model arising in viscoelasticity. Applied Mathematics and Computation 2023; 440:127655
39. Guo T, Nikan O, Avazzadeh Z, and Qiu W. Efficient alternating direction implicit numerical approaches for multi-dimensional distributed-order fractional integro differential problems. Computational and Applied Mathematics 2022; 41:236
40. Qiu W, Nikan O, and Avazzadeh Z. Numerical investigation of generalized tempered-type integrodifferential equations with respect to another function. Fractional Calculus and Applied Analysis 2023; 26:2580–601

10.57647/mathsci.2026.2001.06

41. Nikan O, Molavi-Arabshai SM, and Jafari H. Numerical simulation of the nonlinear fractional regularized long-wave model arising in ion acoustic plasma waves. Discrete & Continuous Dynamical Systems Series S 2021; 14:3685–701

42. Nikan O, Rashidinia J, and Jafari H. An improved local radial basis function method for pricing options under the time-fractional Black–Scholes model. Journal of Computational Science 2025 :102610. DOI: 10.1016/j.aej.2024.10.083

43. Nikan O, Golbabai A, Machado JT, and Nikazad T. Numerical solution of the fractional Rayleigh–Stokes model arising in a heated generalized second-grade fluid. Engineering with Computers 2021; 37:1751–64

44. Nikan O, Rashidinia J, and Jafari H. Numerically pricing American and European options using a time fractional Black–Scholes model in financial decision-making. Alexandria Engineering Journal 2025; 112:235–45

45. Ansari A, Derakhshan M, and Askari H. Distributed order fractional diffusion equation with fractional Laplacian in axisymmetric cylindrical configuration. Communications in Nonlinear Science and Numerical Simulation 2020; 113:106590